

hep-ph/9503353
INLO-PUB-95/04
March 1995,
revised February 1996

Hard Photons in W Pair Production at LEP 2

Geert Jan van Oldenborgh

`gj@rulgm0.leidenuniv.nl`

*Instituut-Lorentz, Rijksuniversiteit Leiden, Postbus 9506, NL-2300 RA Leiden,
Netherlands*

Abstract

The properties of hard photon radiation in W pair production at LEP 2 are studied, with emphasis on the energy loss relevant to the W mass measurement. We use a combination of the exact 1-photon matrix element and leading logarithmic structure functions. Defining unobservable, observable and initial state photons in the phase space, it is shown that neither the one-photon matrix element nor the leading logarithmic structure functions alone give an adequate description of the energy loss due to observable or initial state photons. An event generator based on these calculations is available.

¹ Research supported by the Stichting FOM

1 Introduction

One of the major goals of the LEP 2 experiments is an accurate determination of the mass of the W boson. A comparison of the measured value with the one predicted from other precision electro-weak measurements will serve as a sensitive check of the Standard Model. The most precise measurement method seems to be a constrained fit of the final state in the semi-leptonic (lepton+jets) and hadronic (4 jets) channels. These fits assume that there is no hard radiation or that the photon spectrum is known. Final state radiation can easily be incorporated by adding the photon to the nearest outgoing charged particle, but the shift in the fitted W mass caused by initial state radiation will have to be determined using theoretical input. In particular, in order to get a precision in M_W better than 10 MeV, the average energy loss has to be known to 20–25 MeV.

In W pair production the distinction between initial and final state radiation is not unique (unlike in the case of neutral particles such as the Z boson). In the matrix element, the universal leading logarithmic parts (proportional to $\log(s/m_e^2)$) are easily separable, but the non-universal finite terms do not split naturally (although the current splitting technique [1] seems to achieve a ‘good’ separation). We therefore define initial state radiation in the phase space rather than the matrix element; this is also more in line with the experimental possibilities. We use two definitions. The first is the criterion that the outgoing photon is closer to the beam than to any charged final state particle. The second assumes that events with observable photons are analysed separately, and defines initial state radiation as unobservable photons closer to the beam than to other charges particles; this is almost equivalent to a cone around the beam.

The first computation of hard radiation to off-shell W pair production was performed by Aeppli & Wyler [2]; this calculation did not include mass effects so it could not cover the collinear regions. In Ref. [3] we gave the extension to the full phase space and an event generator. Other event generators contain a leading log description of initial state radiation, like [4–6], where the last two use a shower algorithm to generate p_T and multiple photons. The semi-analytical calculation of Ref. [1] also gives some of the finite terms in the current splitting scheme, which allows for a gauge-invariant separation of initial and final state separation. They include the universal non-resonant graphs. Finally, a first exploration of the hard radiation off the single W (t-channel) graphs of $e^+e^- \rightarrow e^-\bar{\nu}_e u \bar{d} \gamma$ was presented in Ref. [7]. The goal of this article is to give a very good description of hard radiation, including the exact 1γ matrix element at large angles, and the leading $\mathcal{O}(\alpha^2)$ contributions at small angles to the beam. The various definitions of initial state radiation are compared, and the validity of the approximations made by other compu-

tations investigated. The influence of the universal non-resonant diagrams is confirmed to be small; other diagrams leading to some of the 4-fermion + γ final state, such as ZZ graphs, single W production and QCD graphs, have not yet been included.

We start with a technical description of the matrix elements and phase space used. Next we give results for the energy and p_T spectrum of observable, initial state and unobservable radiation, and the average energy loss. This is compared with the same quantities in the one-photon and leading log approximation, and the influence of the universal non-resonant graphs is computed. Finally, we mention where the event generator which incorporates these calculations can be obtained.

2 Method

2.1 Hard Bremsstrahlung

The method used in this calculation is an exact matrix element for the reaction $e^+e^- \rightarrow 4f + \gamma$ convoluted with structure functions to describe multiple collinear photons. The phase space is thus the one-photon phase space (the multi-channel MC described in Ref. [3]) plus collinear photons, the sum of which is represented by one particle in each direction. No attempt has been made to use a shower algorithm to resolve these into individual photons.

We use two matrix elements. The first one is the original massless one of Ref. [2] (explicit expressions for this matrix element are also given in Ref. [8]). Leading mass effects are added as described in Ref. [3]: When the angle between the photon and a charged particle i is so small that the mass effects become significant we use

$$|M_{\text{massive}}|^2 = |M_{\text{massless}}|^2 \frac{(q_i q_\gamma)}{(p_i p_\gamma)} - e^2 \frac{m_i^2}{(p_i p_\gamma)^2} \quad (1)$$

where the q_j denote the massless momenta, and the p_j the massive ones. This way the logarithmically mass singular and finite (m_i^2/m_i^2) terms are included correctly.

The second matrix element, used mainly for cross-checks, has been generated automatically using MadGraph [9]. It is an order of magnitude slower but contains all mass effects without approximations. Using this matrix element one also has the possibility to study the effect of universal non-resonant graphs. The ZZ and single W graphs are also included, but as long as the appropriate

channels have not been added to the phase space mappings these can not be used.²

Given the number of expected events these 1γ matrix elements are accurate enough for a good description of large-angle hard photon emission. However, they fall short in describing the collinear initial state bremsstrahlung, which is dominated by large logarithms $\log(s/m_e^2)$. These can be resummed (and higher order contributions can be included) in structure functions (transition functions) [10–14], but only after integrating out the transverse momentum p_T . As in Ref. [15], we combine these two approaches by only resumming the radiation inside a cone $\theta < \theta_c$; subtracting the leading $\log \mathcal{O}(\alpha)$ part from the explicit matrix element to avoid double counting. This gives multi-photon emission, but only on the side where the explicit photon happened to be.

Using structure functions one would like to write the matrix element as

$$\sigma = \int dk^+ \rho(k^+) \int dk^- \rho(k^-) \frac{|M((1-k^+)(1-k^-)s)|^2}{2(1-k^+)(1-k^-)s}, \quad (2)$$

with k^\pm the fraction of the incoming momentum taken away by collinear initial state radiation off the e^\pm and $M(\hat{s})$ some hard scattering amplitude. We use the structure functions given in Refs [10,16]³

$$\rho(k) = \beta k^{\beta-1} (1 + \delta_1^{V+S} + \delta_2^{V+S}) + \delta_1^H(k) + \delta_2^H(k), \quad (3)$$

with $\beta = \frac{\alpha}{\pi}(L-1)$ and $L = \log(\mu^2/m_e^2)$ the large collinear logarithm. The terms δ denote the infrared finite parts of the leading one- and two-loop corrections:

$$\delta_1^{V+S} = \frac{\alpha}{2\pi} \left(\frac{3}{2}L + \frac{\pi^2}{3} - 2 \right) \quad (4)$$

$$\delta_1^H(k) = \frac{\alpha}{2\pi} (1-L)(2-k) \quad (5)$$

$$\delta_2^{V+S} = \left(\frac{\alpha}{2\pi} \right)^2 \left(\frac{9}{8} - \frac{\pi^2}{3} \right) L^2 \quad (6)$$

$$\begin{aligned} \delta_2^H(k) = & \left(\frac{\alpha}{2\pi} \right)^2 \left[-\frac{1+(1-k)^2}{k} \log(1-k) \right. \\ & \left. + (2-k) \left(\frac{1}{2} \log(1-k) - 2 \log(k) - \frac{3}{2} \right) - k \right] L^2 \end{aligned} \quad (7)$$

² A possible exception is the study of large-angle electrons in the case of single W production, as in Ref. [7].

³ The difference with the 3-loop YFS structure function [17] is $\mathcal{O}(10^{-3})$ in the variables studied.

For the scale we use $\mu^2 = s(1 - \cos \theta_c)/2$, which reproduces the $\mathcal{O}(\alpha)$ results and agrees with the scale usually taken when no cone is defined.

We have to define the hard scattering amplitude in such a way that collinear photon radiation is not included twice, preferably keeping it positive definite. The procedure followed resembles the one described in Ref. [15]. For large angles (larger than θ_c) we take for this amplitude the 1γ matrix element. However, inside the cone we must first subtract from this the $\mathcal{O}(\alpha)$ leading log part which has already been included in the structure functions:

$$|M_{\text{sub}}|^2 = e^2 \left(\frac{1 + (1 - k)^2}{k(1 - k)} \frac{1}{(p_i p_\gamma)} - \frac{m_i^2}{(p_i p_\gamma)^2} \right) |M_0((1 - k)s)|^2. \quad (8)$$

Here $k = E_\gamma/E_e$ and $|M_0|^2$ denotes the matrix element without photon evaluated at a lower energy. This expression only holds strictly in the collinear limit, and breaks down when the cone is chosen too large (typically around 90°).

Next we add again the exponentiated leading log result: the lowest order matrix element times structure function, but now at $k' = k^\pm + x$, with $x = E_\gamma/E_e$ the fraction of the beam energy taken by the explicit photon and the direction (\pm) determined by the direction of the explicit photon:

$$|M_{\text{add}}((1 - k^+)(1 - k^-)s)|^2 \stackrel{\theta_\gamma \leq \theta_c}{=} S \int_{E_{\text{min}}/E_e} dx \frac{|M^{(0)}((1 - k^\mp)(1 - k'))|^2}{1 - k'} \frac{\rho(k')}{\rho(k^\pm)} \frac{g(x, k')}{\int_{E_{\text{min}}/E_e}^{k'} dx' g(x', k')}. \quad (9)$$

$g(x, k')$ is an arbitrary function and S a symmetry factor defined later. In order to get roughly the same behaviour as the original matrix element we choose

$$g(x, k') \approx \frac{1}{1 - k'} \rho(k' - x) \rho_2(x/(1 - k' + x)), \quad (10)$$

with $\rho_2(x)$ the function $\rho(x, \alpha \rightarrow 2\alpha)$ which approximates the matrix element squared in one direction. We use an approximation as the function has to be analytically integrable.

However, this is only half the story, as the lower bound on the photon energy is now always imposed on the side on which the explicit photon happened to be. The region in phase space where the collinear photon on the other side has satisfied this bound, $k^\mp E_e > E_{\text{min}}$, is included by defining $S = 2 - \theta(E_{\text{min}} - k^\mp E_e)$. The step function avoids double counting when both collinear photons

have large energies. The total matrix element is then given by

$$|M_{\text{full}}|^2 = |M_{\text{massive}}|^2 - |M_{\text{sub}}|^2 + |M_{\text{add}}|^2 \quad (11)$$

The collinear energy lost in the forward and backward directions is the sum of many photons. We can approximate the p_T of this bunch of collinear photons by the p_T spectrum of a single photon of the same energy to obtain a smooth transition from the 1γ matrix element to the exponentiated one. The resulting violations of energy-momentum conservation are of order $E_\gamma \sin^2 \theta$, and hence negligible for small cone sizes. The implementation of a true parton shower algorithm [5] is foreseen for the near future.

The same subtraction of the leading logarithmic contribution can be performed for final state photons. As the exact difference between a single fermion and a fermion accompanied by collinear photons is not important for most measurements, we have not performed the exponentiation as we did for the initial state photons. Also, radiation off a hadronic final state is badly described by the radiation of an on-shell quark: the effective mass of the radiating particle is the mass of the whole jet, not the on-shell mass of a naked quark. This reduces the bremsstrahlung considerably. In the time domain this means that the quark will radiate off gluons before it can radiate off a photon; the amount of hard radiation near a jet is thus overestimated. The possibility to turn off the final state radiation means that one can leave the generation of these photons to more heuristic algorithms (see, e.g., [6]) tuned to the observed spectrum if this spectrum is important.

An unsolved problem is the matter of gauge invariance of bremsstrahlung off unstable particles. As we use a constant width in our calculations the current is conserved (the substitution $p_\gamma^\mu \rightarrow \epsilon_\gamma^\mu$ gives zero), but this is not sufficient to guarantee gauge invariance. However, there are no cancellations which could amplify the gauge violating terms, so we expect the effects to be small. A test using the inclusion of triangle graphs is being performed.

2.2 Soft Bremsstrahlung

In the following we will consider mainly the average energy lost by photons,

$$\langle E_\gamma \rangle = \frac{1}{\sigma_0^{\text{isr}}} \int dE_\gamma E_\gamma \frac{d\sigma}{dE_\gamma} \quad (12)$$

The normalisation σ_0^{isr} is computed from the tree level matrix element for the reaction $e^+e^- \rightarrow 4$ fermions, convoluted with structure functions. This has an

accuracy of a few percent. However, as an overall factor it will not influence the conclusions very much.

In the case of a strict one-photon calculation the integral in Eq. 12 is not sensitive to soft photons, and we can make accurate predictions without knowing the virtual and soft corrections. However, when we add the possibility of multiple photon emission through the procedure given above, and define E_γ as the *sum* of the photon energies, these do play a role. Note that we consider the regime $E_{\min} \ll \Gamma_W$. In this case the soft corrections are easily found to be

$$|M_{\text{soft}}|^2 = e^2 \sum_{i,j} Q_i Q_j B(p_i, p_j; E_{\min}, \lambda) |M_0|^2, \quad (13)$$

with Q_i the charges of the particles in terms of the unit charge e . The function

$$B(p_i, p_j; E_{\min}, \lambda) = \pm \frac{(p_i p_j)}{(2\pi)^3} \int_{E_\gamma < E_{\min}} \frac{d^3 p_\gamma}{2E_\gamma} \frac{1}{(p_i p_\gamma)} \frac{1}{(p_j p_\gamma)} \quad (14)$$

is given in Ref. [18] (the sign depends on whether the particles are incoming or outgoing). It depends logarithmically on the infra-red regulator, for which we use a small photon mass λ . We can include the corresponding infra-red logarithms of the virtual corrections by the substitution $\lambda \rightarrow \mu_{\text{IR}}$. We choose for this scale $\mu_{\text{IR}} = M_W/n$, with n the number of charged final state particles. With this heuristic, the difference in the total cross section between the full result and the leading logarithmic approximation is less than 1.5% in the region $175 < \sqrt{s} < 205$.

Both the soft and virtual corrections will contain logarithms in the virtuality of the W bosons, $\log(p^2 - M_W^2 + iM_W \Gamma_W)$. However, these cancel in the sum. This can be seen in the hard photon spectrum (Figs 1–3) as an absence of a kink at $E_\gamma \approx \Gamma_W$. The cut-off on the initial-final and final-final state interference as the energy increase is thus exactly compensated by the emergence of radiation off the W bosons.

We also extract the Sudakov double logs

$$|M_{\text{sud}}|^2 = \frac{e^2}{(2\pi)^2} \sum_i Q_i^2 \log^2 \frac{m_i}{\mu_{\text{IR}}} |M_0|^2. \quad (15)$$

When we introduce the structure functions we have to subtract again the part which would be double-counted:

$$|M_{\text{sub,soft}}|^2 = \frac{e^2}{2\pi^2} [2(L-1) \log \frac{2E_{\min}}{\sqrt{s}} + \frac{3}{2}L + \frac{\pi^2}{3} - 2] \quad (16)$$

The tree term has already been added to the hard radiation for $E_\gamma > E_{\min}$, we need to add it only to the soft terms as

$$|M_{\text{tree}}|^2 = (1 - \theta((k_{\min} - k^+)(k_{\min} - k^-))|M_0|^2 \quad (17)$$

Adding all up the estimate for the non-radiative part is

$$|M_{\text{full,soft}}|^2 = |M_{\text{soft}}|^2 - |M_{\text{sud}}|^2 - |M_{\text{sub,soft}}|^2 + |M_{\text{tree}}|^2 \quad (18)$$

The other terms in the virtual corrections do not contain large logarithms, and are thus expected to be of order $\alpha/\pi \lesssim 1\%$. As they only enter as corrections to the main effects of hard radiation in the quantities studied in this paper this is negligible. For the factorizable graphs, for which the off-shell result is under study, this reproduces the full result to a few percent in the cross section. A change in the scale μ_{IR} of a factor 2 gives a difference of 3% in the cross section, but only 1% in the observable energy (where the effect of the virtual and soft terms is much smaller). We verified that the numbers obtained with this soft matrix element did not any more depend on the cut-off E_{\min} .

3 Results

We now turn to the predictions we can make for the hard photon spectrum in W pair production. We first define the ‘LEP 2 canonical cuts’ that are used to compute observables that can easily be compared to other calculations. These cuts also give an impression what an actual experiment could observe. Next we show the energy and p_T spectrum for observable and initial state photons. This can be compared with the one-photon approximation on the one hand, and the leading log approximation on the other. Finally we discuss the effect of the non-resonant diagrams.

The canonical cuts of the ADLO/TH detector [19] are given in Table 1. τ ’s are not considered. The cuts on the photon separations should be interpreted as follows: first each photon is combined with the nearest charged particle if the angle to it is smaller than 5° (outgoing) or 1° (beam); combining with the beam means dropping it. Next all the other cuts are applied. This way spurious collinear divergences near cuts are avoided.

Observable photons are defined as those which pass these cuts. Unobservable initial state photons are the ones cut out by the energy cut or the minimum angle to the beam; the sum of their energies and p_T can be deduced from momentum conservation. Finally, we define initial state photons to be the

separation	γ	e	μ	jet	acceptance	E_{\min}	θ_{\min}
γ	5°	5°	5°	5°	γ	0.1 GeV	1°
e	5°	5°	5°	5°	e	1 GeV	10°
μ	5°	5°	5°	5°	μ	1 GeV	10°
jet	5°	5°	5°	5 GeV	jet	3 GeV	0°

Table 1
Canonical cuts

unobservable ones plus observable photons which are closer to the beam than to any other charged particles.

In the subsequent part of this work we use the following parameters. We work in the G_μ scheme, but with the coupling of the extra photon determined by $\alpha(\mu^2 = 0)$. All masses are taken from the Particle Data Group 1994 edition [20]. The quark masses were taken $m_u = 63$ MeV, $m_d = 83$ MeV, $m_s = 215$ MeV and $m_c = 1.5$ GeV for compatibility with the virtual off-shell calculation. The W mass is 80.23 GeV. The W width is computed in leading order, with the strong coupling constant $\alpha_s = 0.117$; this gives $\Gamma_W = 2.081$ GeV. To conserve the electromagnetic current we use a fixed W width; the pole position is computed as $\mu_W = M_W^2 - \Gamma_W^2 - 5/2\pi \Gamma_W^3/M_W - iM_W\Gamma_W - i\Gamma_W^2/pi + i(1 - 1/pi^2)\Gamma_W^3/M_W$. The Z width is neglected, and the energy of the outgoing photon restricted to less than $E - (M_Z + 5\Gamma_Z)^2/4E$ to avoid the Z peak.⁴ Unless otherwise noted we assumed a beam energy of 87.5 GeV. We used a cone angle of 10°. Changing this to 5° shifts the observables by an amount comparable to the integration accuracy, $\mathcal{O}(1\%)$.

The results are presented in Figs 1–3 and Tables 2 and 3. First we give the observable tree level non-radiative cross section (σ_0), the same convoluted with leading log structure functions (σ_0^{isr}) and with non-resonant graphs ($\sigma_{0+\text{nr}}^{\text{isr}}$). For the next entries we consider the full calculation described in section 2, the exact one-photon matrix element (1γ) and the leading log result (LL). For technical reasons the leading logarithmic approximation can only be computed for photons emitted in the forward direction ($\theta_c = 90^\circ$), so the scale is taken to be $\mu^2 = s/2$. This will underestimate the leading log result. We also give the full result including the universal non-resonant diagrams (full+nonres). The statistical errors on the cross sections are $\mathcal{O}(0.1\%)$, but the differences (LL – full) and ((res + nonres) – res) were computed directly in this form and have relative errors of a few percent and a few tens of percents respectively on these differences. The statistical errors on the the average photon energies are slightly larger, 0.3–0.5%. We introduced an upper cut-off on the photon energy to avoid the Z peak, this influences only the observable average energy.

⁴ The cross section above this cut is entirely negligible [2].

For the normalisation we need the total cross section for W pair production. As long as the full off-shell one-loop result is not yet available we use the lowest order cross section with leading logarithmic structure functions. As the final state corrections cancel against the corrections to the width, and the initial-final interference is expected to be of order $\alpha\Gamma_W$ this is a reasonable approximation. This uncertainty only affects the overall normalisation of the results, not the differences between the different results. The main effect of the initial state radiation is of course to lower the result, as we are just above the threshold for W pair production and phase space is limited. The contribution from the non-resonant graphs is negligible in this energy range (as had already been observed in Ref. [2]). With the scale choice used, the full result deviates from this estimate by less than 1.5%.

One can see from the Tables that an appreciable fraction (around one quarter) of the events will be accompanied by photons observable in the ADLO/TH set of cuts. This is due to the excellent forward coverage ($\theta_\gamma > 1^\circ$) and electromagnetic calorimeter ($E_\gamma > 0.1$ GeV) assumed in the canonical cuts. Reducing the angle to 10° this fraction still is around 20%, of which half also has an $E_\gamma > 1$ GeV. For the W mass measurement it would be advantageous to make use of the extra information present and analyse these events separately. Neither the 1γ matrix element nor the leading log approximation give a satisfactory description of the observable photons. By radiating only one photon one effectively normalises to the non-radiative lowest order, which is too large. On the other hand, the leading log approximation misses the negative initial-final state interference terms ($E_\gamma \lesssim \Gamma_W$) and the radiation off the (off-shell) W bosons (mainly when $E_\gamma \gtrsim \Gamma_W$).⁵ Finally, given that the un-exponentiated large-angle contribution of the cross section still is 20% of the total cross section the region $E_\gamma < 1$ GeV should not be trusted to 1% even in the full calculation. Most of the cross section here is, however, associated with the final state and hence does not influence the W mass measurement.

The observable photon energy is dominated by final state radiation and hence not very interesting. The unobservable energy spectrum is much more independent of the final state. It is not completely independent due to the possibility of observable jets in the beam pipe ($\theta_j = 0^\circ$). The initial state radiation associated with these events is sometimes associated with the final state by the canonical cuts, thus lowering the average energy. As the radiation off jets is not modelled correctly anyway, a cut will have to be imposed to exclude this contamination. One sees that analysing observable photons separately reduces the average energy loss, and hence the size of the theoretical corrections to be applied to the fitted W mass. The difference in $\langle E_\gamma^{\text{isr}} \rangle$ is due to the amount of

⁵ The fact that there is no discernible structure at $E_\gamma \approx \Gamma_W$ in Fig. 1 suggests that these two contributions are intimately connected; indeed, one cannot define the ‘radiation off the W ’ in a gauge invariant way.

phase space available: 2, 3 or 4 charged particles. For the unobservable radiation the leading log approximation is, as expected, quite good⁶. As in the total cross section, the contribution of the non-resonant graphs is not visible due to the limited integration accuracy. The contributions from the universal non-resonant graphs cannot be distinguished from the statistical fluctuations,⁷ but may just be relevant. At 205 GeV the integrated radiative corrections are smaller, but as there is much more phase space for the photons, more can be observed. The same remarks on the accuracy of the various approximations hold here, except that the deviations tend to be larger.

4 Conclusions

We have studied the properties of hard radiation in W pair production at LEP with a combination of the exact matrix element for one-photon emission and resummed structure functions for the initial state collinear large logarithms. We find that a large fraction of the W events will be accompanied by observable hard photons; a separate analysis of these events should decrease the systematic errors in the W mass measurement. These events are not well described either by the 1γ matrix element or a pure leading log approximation. The treatment of photons near jets is an unsolved problem.

The average energy lost by the remaining, unobservable photons is smaller. The canonical LEP 2 cuts leave a contamination of final state radiation due to the inclusion of jets down to the beam pipe, which will have to be removed. In this region of phase space, a leading log treatment is adequate. We have not yet addressed the issues of radiation off non-resonant graphs other than the (probably negligible) universal ones; in particular the QCD, ZZ and single W graphs have not yet been included.

An event generator based on the calculations presented in this article can be obtained from `ftp://rulg4.LeidenUniv.nl/pub/gj` or via the World Wide Web.

⁶ The systematic shift for leptonic, semi-leptonic and hadronic channels is probably due to the choice of the scale μ_{IR} , which should be slightly different for the different final states considered.

⁷ The numbers presented here are based on $2.5 \cdot 10^5$ weighted events per channel and took about 100 hours in all to compute on a fast workstation.

Acknowledgements

I would like to thank Niels Jørgen Kjaer and Willy van Neerven for comments on the manuscript and useful discussions, and the NIKHEF in Amsterdam for the use of their computers.

References

- [1] D. Bardin, A. Olchevskii, M. Bilenkii and T. Riemann. Phys. Lett. **B308** (1993) 403.
- [2] A. Aepli and D. Wyler. Phys. Lett. **B262** (1991) 125.
- [3] G. J. van Oldenborgh, P. J. Franzini and A. Borrelli. Comp. Phys. Comm. **83** (1994) 14.
- [4] F. A. Berends, R. Pittau and R. Kleiss. Nucl. Phys. **B426** (1994) 344.
- [5] H. Anlauf, J. Biebel, A. Himmeler, P. Manakos, T. Mannel, W. Schonau and H. D. Dahmen. Comput. Phys. Comm. **79** (1994) 487.
- [6] T. Sjostrand. Comp. Phys. Comm. **82** (1994) 74.
- [7] J. Fujimoto, S. Ishikawa, Y. Kurihara, Y. Shimizu and D. Perret-Gallix. Non-resonant Diagrams in Radiative Foru-Fermion Processes. In Physics at LEP200 and Beyond, Teupitz, 1995. DESY/Zeuthen.
- [8] A. Aepli. Radiative Corrections in the Electroweak Theory. Ph.D. thesis, University of Zürich, 1991.
- [9] T. Stelzer and W. F. Long. Comput. Phys. Commun. **81** (1994) 357.
- [10] F. A. Berends, W. L. van Neerven and G. J. H. Burgers. Nucl. Phys. **B297** (1988) 429. Err. Nucl. Phys. **B304** (1988) 95.
- [11] E. A. Kuraev and V. S. Fadin. Yad. Fiz. **41** (1985) 753. (*Sov. J. Nucl. Phys.* **41** (1985) 466).
- [12] G. Altarelli and G. Martinelli. In Physics at LEP, Edited by J. Ellis and R. Peccei, Genève, 1986. CERN 86-02.
- [13] O. Nicrosini and L. Trentadue. Phys. Lett. **196B** (1987) 551.
- [14] R. Kleiss. Nucl. Phys. **B347** (1990) 67.
- [15] J. Fleischer, F. Jegerlehner, K. Kołodziej and G. J. van Oldenborgh. Comp. Phys. Comm. **85** (1994) 29.
- [16] J. Fleischer, K. Kołodziej and F. Jegerlehner. Phys. Rev. **D47** (1993) 830.

$$E_{\text{beam}} = 87.5 \text{ GeV}$$

	leptonic	semi-leptonic	hadronic
$\sigma_0[\text{pb}]$.724 (20%)	4.564 (20%)	7.132 (20%)
$\sigma_0^{\text{isr}}[\text{pb}]$.604	3.803	5.944
$\sigma_{0+\text{nr}}^{\text{isr}}[\text{pb}]$.605 (.13%)	3.808 (.14%)	5.952 (.14%)
$\sigma^{\text{obs}}/\sigma_0^{\text{isr}}$			
full	.280	.265	.242
1γ	.359 (28%)	.322 (21%)	.297 (23%)
LL	.292 (4.2%)	.273 (2.9%)	.245 (1.2%)
with nonres	.281 (.17%)	.265 (.10%)	.242 (.08%)
$\langle E_\gamma^{\text{obs}} \rangle [\text{GeV}]$			
full	1.247	1.013	.777
1γ	1.414 (.167)	1.145 (.132)	.884 (.107)
LL	1.265 (.018)	1.039 (.025)	.814 (.037)
with nonres	1.245	1.012	.776
$\langle E_\gamma^{\text{unobs}} \rangle [\text{GeV}]$			
full	.666	.665	.647
1γ	.864 (.198)	.856 (.191)	.857 (.210)
LL	.663 (−.003)	.659 (−.007)	.657 (.010)
with nonres	.665	.665	.646
$\langle E_\gamma^{\text{isr}} \rangle [\text{GeV}]$			
full	1.223	1.174	1.063
1γ	1.488 (.264)	1.419 (.245)	1.320 (.257)
LL	1.208 (−.015)	1.176 (.002)	1.088 (.025)

Table 2

Cross section for observable photons and energy lost to observable, unobservable and initial state photons at $\sqrt{s} = 175 \text{ GeV}$.

[17] M. Skrzypek and S. Jadach. Z. Phys. **C49** (1991) 577.

[18] G. 't Hooft and M. Veltman. Nucl. Phys. **B153** (1979) 365.

[19] F. Cavallari, J. Gascon, M. Grünewald, N. Kjaer, T. Ohl and J. Schwindling. Canonical Cuts for Benchmarking LEP2 Monte Carlos. Available on the web as <http://hpl3rm06.roma1.infn.it/user/cavallari/www/tran/cc.ps>.

[20] Particle Data Group (L. Montanet, et al). Phys. Rev. **D50** (1994) 1173.

$$E_{\text{beam}} = 102.5 \text{ GeV}$$

	leptonic	semi-leptonic	hadronic
$\sigma_0[\text{pb}]$.831 (7%)	5.280 (8%)	8.316 (8%)
$\sigma_0^{\text{isr}}[\text{pb}]$.774	4.908	7.724
$\sigma_{0+\text{nr}}^{\text{isr}}[\text{pb}]$.774 (.07%)	4.912 (.08%)	7.730 (.08%)
$\sigma^{\text{obs}}/\sigma_0^{\text{isr}}$			
full	.295	.289	.267
1γ	.354 (20%)	.326 (13%)	.302 (13%)
LL	.317 (7.2%)	.303 (4.9%)	.276 (3.3%)
with nonres	.296 (.08%)	.289 (.08%)	.268 (.02%)
$\langle E_\gamma^{\text{obs}} \rangle [\text{GeV}]$			
full	2.010	1.802	1.555
1γ	2.106 (.096)	1.830 (.028)	1.593 (.038)
LL	2.084 (.074)	1.853 (.051)	1.599 (.044)
with nonres	2.008	1.801	1.554
$\langle E_\gamma^{\text{unobs}} \rangle [\text{GeV}]$			
full	1.902	1.923	1.884
1γ	2.266 (.364)	2.240 (.316)	2.241 (.357)
LL	1.866 (−.035)	1.880 (−.044)	1.875 (−.009)
with nonres	1.900	1.922	1.882
$\langle E_\gamma^{\text{isr}} \rangle [\text{GeV}]$			
full	3.168	3.147	2.976
1γ	3.549 (.380)	3.447 (.300)	3.344 (.368)
LL	3.156 (−.013)	3.106 (−.041)	2.992 (.017)

Table 3

Cross section for observable photons and energy lost to observable, unobservable and initial state photons at $\sqrt{s} = 205 \text{ GeV}$.

Figures

Inclusion of the universal non-resonant graphs gives curves which are indistinguishable from the ‘full’ calculations. The wiggles are due to the limited statistical accuracy (10^7 weighted events per curve).

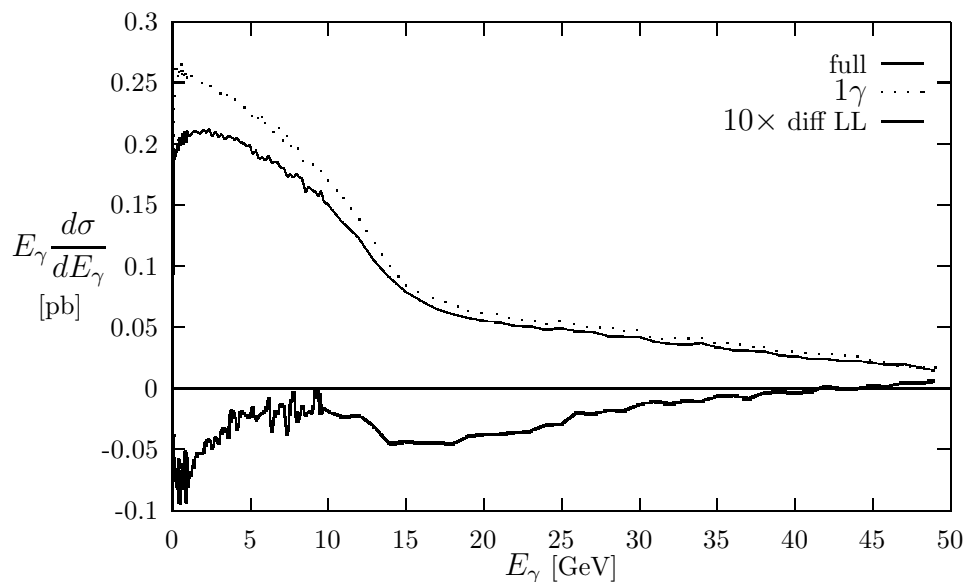


Fig. 1. Observable photon energy in the semi-leptonic channel.

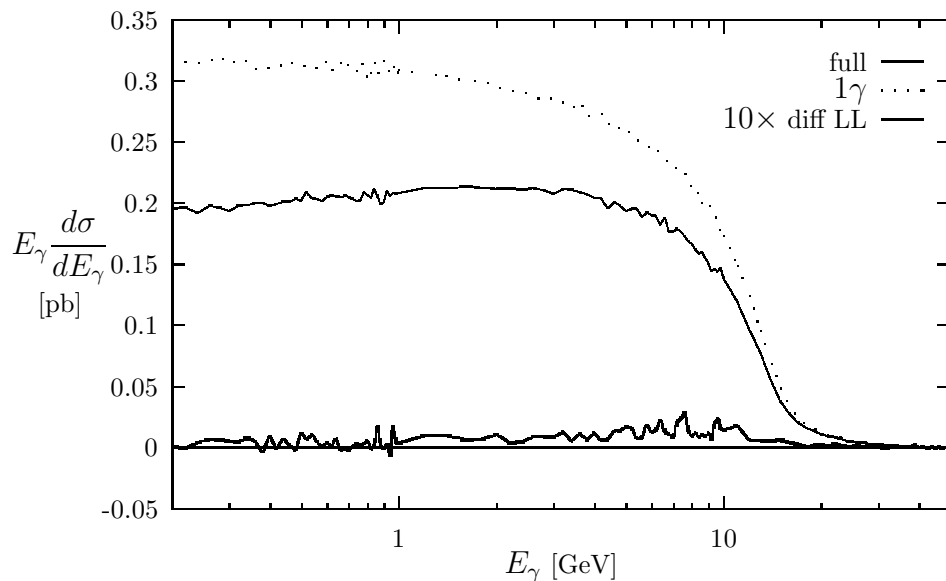


Fig. 2. Unobservable photon energy in the semi-leptonic channel.

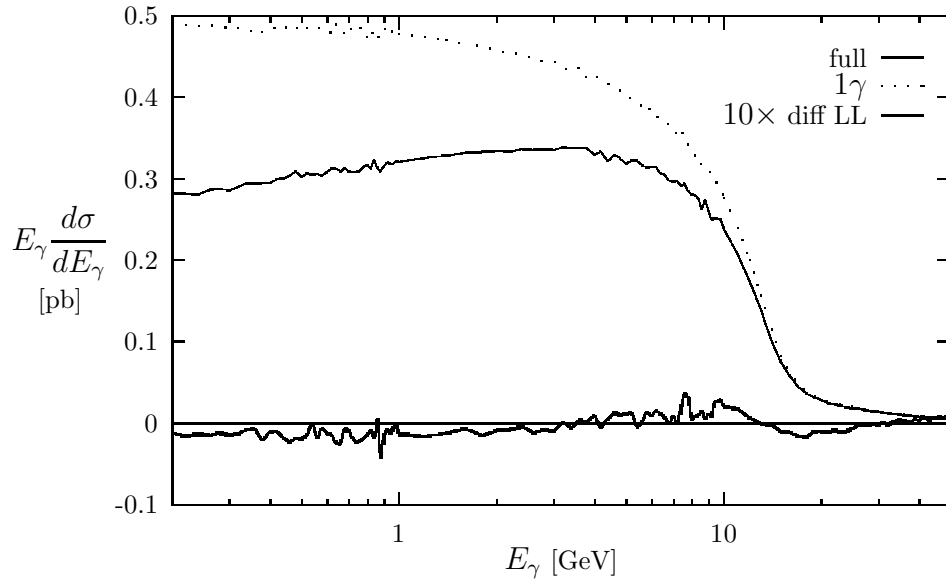


Fig. 3. Initial state photon energy in the semi-leptonic channel.